



ELSEVIER

Available online at www.sciencedirect.com

Information Fusion xxx (2006) xxx–xxx

INFORMATION
FUSIONwww.elsevier.com/locate/inffus

Image enhancement through intelligent localized fusion operators in the automated visual inspection of highly reflective surfaces

Aureli Soria-Frisch ^{a,*}, Mario Köppen ^b^a *Technology Department, Pompeu Fabra University, Passeig Circumval·lació 8, 08003 Barcelona, Catalonia, Spain*^b *Fraunhofer IPK, Department of Security Technologies, Pascalstr. 8-9, 10587 Berlin, Germany*

Received 15 November 2004; received in revised form 30 August 2006; accepted 30 August 2006

Abstract

The selection of a suitable illumination subsystem is seldom practicable in the automated visual inspection of highly reflective surfaces. The paper presents an algorithmical approach in the form of a framework for enhancing images of objects with such surfaces. This framework is based on the application of so-called Intelligent Localized Fusion Operators (ILFOs), whose formalization is herein undertaken for the first time. Furthermore the guidelines for its implementation are given and different aspects of the resulting pre-processing system are systematically analyzed. The framework successfully performs in the automated visual inspection of different objects presenting highly reflective surfaces, namely headlamp reflectors, plastic bundled packages, and electric bulbs.

© 2006 Published by Elsevier B.V.

Keywords: Fuzzy integral; Fuzzy measures; Image enhancement; Image processing

1. Introduction

The automated visual inspection of objects with highly reflective surfaces results extremely complex due to the presence of some areas in the acquired images, where the camera detector is saturated. These areas are known as highlights. Though this problem can be tackled by applying a suitable lighting system, this solution is not trivial and seldom practicable for such objects. In this context the application of a pre-processing system for filtering the highlights becomes extremely helpful.

Following the seminal paper of Burt and Kolczynsky [1] image fusion has been applied for image enhancement in different applications. In [1] an image pyramid is used in order to fuse a multi-focal image set through a weighted sum operator. On the other hand, the active consideration of the illumination conditions in the image acquisition pro-

cess in order to obtain a well-conditioned input image was taken into consideration in [2] for the first time. As an extension of these two works, some research groups [3–5] apply image fusion on a multi-dimensional image set resulting from different illumination conditions in order to enhance it.

The framework proposed in [3] is based on a model-based approach for the evaluation of the fused image energy [6]. Different images taken under varying illumination conditions are fused within a probabilistic Bayesian framework, where the employed fusion operator can be modeled as a weighted sum. The second approach [4] applies a so-called comparometric processing of an image set taken under different exposure times. The used comparometric equations are related to the fields of photometry and radiometry. They are applied in order to increase the signal-to-noise ratio of the output image. Thus, the image fusion results from the application of diverse non-linear functions.

In the framework presented in [5] a multi-dimensional set of images taken under different illumination conditions

* Corresponding author. Tel.: +34 93 5422564; fax: +34 93 5422517.
E-mail address: aureli.soria-frisch@ieee.org (A. Soria-Frisch).

are fused with a so-called Intelligent Localized Fusion Operator (ILFO), which is a further development of the fuzzy integral [7] within a theoretical framework denoted as soft data fusion [8,9]. This theoretical framework focus its attention on the role of the operator binding the data from the different information sources in multi-sensory systems. In this context, the fuzzy integral, which presents a non-linear function for the fusion of information, plays a principal role because it generalizes the more common fusion operators. Thus it subsumes the weighted sum approach employed in [1,3]. In contrast to the other non-linear methodology proposed in [4], ILFOs improve the interpretability of the fusion operator because of its relationship to the field of Fuzzy Computing. The framework presented in [5] attains for the first time the filtering of highlights as a pre-processing task in automated visual inspection, whereas the frameworks in [3,4] attain the general image enhancement of the input images.

The here presented paper furthers the framework based on ILFOs [5]. The formalization and the automation of different aspects of the framework is undertaken herein for the first time. The formalization succeeds by taking the Theory of Fuzzy Sets [10] and the Pattern Recognition approach presented by Watanabe [11] into account. Moreover, the novel application of peak dynamic analysis [12] for the automation of the process allows the framework to attain the results without heuristic parameterization. This fact constitutes a clear advance with respect to the framework presented in [5]. Although some results could look the same as those obtained in [5], the application of genetic algorithms [13] is newly done herein. In [5] the best results were obtained through the manual modification of the parameters deliver by the genetic algorithms. No manual adaptation is undertaken herein. Furthermore, the following properties of the framework are analyzed herein: automation, best parameterization and convergence of GAs, execution time, generalization capability, and quantitative evaluation of the resulting images' quality. The employment of Interactive genetic algorithms [14] is presented herein for the first time as an alternative to GAs.

The paper is organized as follows. Section 2 gives an overview of the theoretical background on the fuzzy integral, including the more general framework of soft data fusion and some considerations on the application of the fuzzy integral for image fusion. The formalization of ILFOs is attained in Section 3. The pre-processing framework, which is based on the application of an ILFO for highlights filtering is presented in Section 4. The results obtained by applying this framework in different automated inspection systems can be found in Section 5, where the inspection of automotive headlamp reflectors, plastic bundled objects, and electric bulbs is described. The first application is used in order to undertake the systematic analysis of the framework. Finally the conclusions are given in Section 6.

2. Theoretical background

2.1. Soft data fusion and the fuzzy integral

The theoretical framework of soft data fusion [8,9] relate different fusion operators by taking the flexibility of the operation result into account. In this sense traditionally used fusion operators can be considered as hard. Fuzzy fusion operators were established as generalizations of classical ones. This mathematical generalization can be considered as a softening process of the operator, which improves the mentioned flexibility.

The consequence of the evolution of fusion operators from harder to softer ones is shown in the following paragraph. In classical operators the fusion result exclusively depends on the value being operated on. For instance the result of the sum operator just depends on the summands and thus $1.9 + 3.1$ is always computed to 5, different from values "close to 5" like 4.9. The result of such a fusion operation through the application of a softer operator, i.e. a weighted sum, an Ordered Weighted Averaging [15], or a Fuzzy Integral [7], differs from this hard one. This difference is based on the inclusion of an increasing number of freedom degrees in the operators as shown in [9]. While in weighted operators the weight of the information sources is established upon its index, weighted order operators establish the weight upon the ranking of the information sources. This difference improves the performance of the operation w.r.t. compatibility, partial aggregation, and reinforcement [16].

Fuzzy integrals further increase the flexibility of the operator by taking the fusing values, the *a priori* importance of the fusing sources, and their ranking into consideration in the fusion result. This can be observed on hand of the mathematical expression of the Choquet Fuzzy Integral (CFI):

$$\mathcal{C}_\mu[h_1(x_1), \dots, h_n(x_n)] = \sum_{i=1}^n h_{(i)}(x_i) \cdot [\mu(A_{(i)}) - \mu(A_{(i-1)})] \quad (1)$$

where $\mu(A_{(i)}) = \mu(\{x_{(1)}, \dots, x_{(i)}\})$ denote the coefficients of so-called fuzzy measures μ and $h_{(i)}(x_i)$ the fuzzified information sources. The enclosed sub-index states for the ranking result, i.e. $x_{(1)} \geq x_{(2)} \geq \dots \geq x_{(i)}$. This operation determines the coefficients of the fuzzy measures employed in the integration. The reader is referred to [9,17] for a deeper description of this operator.

The fuzzy measure coefficients are used for quantifying the *a priori* importance of the information sources. Fuzzy measures μ are functions on the power set of information sources $\mathcal{P}(X)$, whose coefficients are defined in the interval $[0, 1]$ and fulfill the so-called monotonicity condition:

$$A_j \subset A_k \rightarrow \mu(A_j) \leq \mu(A_k) \quad \forall A_j, A_k \in \mathcal{P}(X) \quad (2)$$

The fuzzy measure coefficients of the subsets with cardinality one are denoted as fuzzy densities $\mu(\{x_i\}) = \mu_i$. They

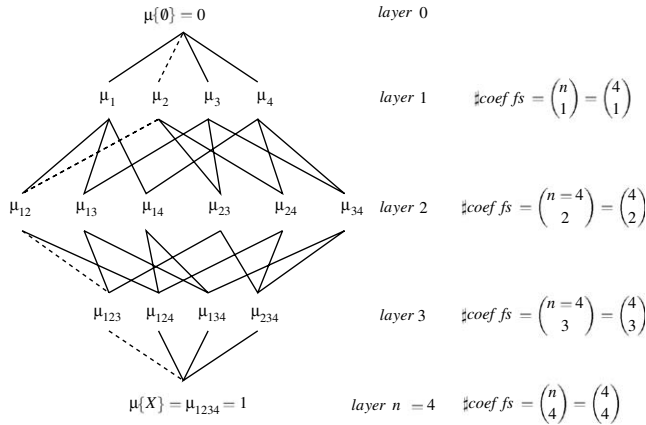


Fig. 1. Lattice structure of a fuzzy measure up to [18]. The data structure constitutes a graph with unidirectional links from $\mu\{\emptyset\}$ to $\mu\{X\}$. The sorting operation of the fuzzy integral, Eq. (1), fixes up the path for the selection of the fuzzy measure coefficients. For instance a dotted line marks the path for the coefficients selected if $x_2 > x_1 > x_3 > x_4$, since then $x_{(1)} = x_2$, $x_{(2)} = x_1$, $x_{(3)} = x_3$, and $x_{(4)} = x_4$.

167 quantify the importance of the individual sources. The
168 remaining coefficients $\mu(\{x_i, \dots, x_j\}) = \mu_{i..j}$ quantify the
169 importance of the coalitions among them [17].

170 2.2. The fuzzy integral in image processing

171 The complexity of fuzzy measures makes a lattice struc-
172 ture suitable for its implementation [18]. Such a graph
173 structure (see Fig. 1) presents $n + 1$ layers, where n is the
174 number of information sources, connected by unidirec-
175 tional links. The nodes of the graph are occupied by the
176 coefficients corresponding to each of the subsets of $\mathcal{P}(X)$.

177 Each layer is occupied by the $\binom{n}{i}$ coefficients that corre-
178 spond to the subsets with the same cardinality. The links
179 connect the subsets among the different layers that satisfy
180 the monotonicity condition (2) of the fuzzy measure. The
181 employment of look-up tables constitutes an alternative
182 to this data structure which can help optimizing the com-
183 putational cost of the fuzzy integral operator.

184 An algorithm of the fuzzy integral for image fusion is
185 presented (see Algorithm 1). The algorithm makes use of
186 the lattice structure formerly presented. Thus, the fuzzy
187 integral is iteratively computed by following the links in
188 the lattice. The used T- and S-norms are defined by the type
189 of fuzzy integral employed [19]. As it can be observed, the
190 fuzzy integral is computed on each pixel of the multi-sen-
191 sory input image in order to fuse the n image channels into
192 a single one.

193 3. Intelligent localized fusion operators

194 Operators for soft data fusion can achieve a higher
195 degree of softness (see Section 2.1) in Image Processing
196 by defining local application domains of the weighting

schemes. This is attained within the paradigm denoted as
Intelligent Localized Fusion (ILF) [20].

Algorithm 1. Iterative algorithm for image fusion through
the fuzzy integral. The algorithm makes use of the lattice
structure of fuzzy measures (see Fig. 1).

```

construct a fuzzy measure  $FM$ 
for all pixels  $P$  in multi-channel image do
     $FI \leftarrow 0$ 
    current node  $\leftarrow \mu\{\emptyset\}$ 
5:    $\mu_{current} \leftarrow 0$ 
    sort pixel channels
    for all element  $CH$  in sorted sequence do
         $\mu_{prior} \leftarrow \mu_{current}$ 
        follow link in lattice corresponding to the current
        element
10:    $\mu_{current} \leftarrow$  coefficient in current node
        if Choquet Integral then
             $\mu_{current} \leftarrow \mu_{current} - \mu_{prior}$ 
        end if
         $TR \leftarrow Tnorm(CH, \mu_{current})$ 
15:    $FI \leftarrow Snorm(FI, TR)$ 
    end for
     $P \leftarrow FI$ 
end for
    
```

Usually the fuzzy measure coefficients are defined by
taking the image as a unit (see Section 2.2). In contrast with
this fact the used fuzzy measure is said to be “localized” in
the ILF paradigm. A “localized” fuzzy measure μ is defined
as a set of fuzzy measures μ^j . Each element of this set oper-
ates on a particular area j of the image domain. The map-
ping between μ^j and the image sub-domain where it
operates is defined through a label image. A fuzzy integral
operated with respect to such locally defined fuzzy mea-
sures becomes a so-called Intelligent Localized Fusion
Operator, ILFO. It is noteworthy to take into consider-
ation how ILFOs are mathematically defined and how they
can be implemented in engineering systems. This is attained
in the following subsections.

3.1. ILFOs’ mathematical foundations

The image space X is partitioned by the label image in
different subspaces X^j , where different fuzzy measures μ^j
are defined. A mapping is then established between j and
the gray-level of the labels g_j .

The definition of the fuzzy measures μ^j attains the charac-
terization of different importance relationships among the
image channels in the corresponding subspaces. The image
space is partitioned based on a process of feature analysis.
The goal of this feature analysis procedure is the determina-
tion and extraction of a set of features, whereby the impor-
tance of the information channels can be established.
Thence the label image codifies the spatial distribution of

255 the analyzed features over the different channels of the input
256 image.

257 The generation of the label image can be formalized as
258 follows. For the sake of simplicity the description is made
259 for a two channel image ($x_i, i = 1,2$). Being the image space
260 $X = \{X_1, X_2\} \rightarrow G^2$, where $g \in [0,255]$ for 8-bit grayvalue
261 images, a feature extraction procedure is applied on each
262 channel X_i . Thus a feature (or a group of them) *a priori*
263 characterizing the importance for the fusion operation is
264 firstly extracted, what can be expressed as $X \rightarrow F$. Thence
265 the application of a threshold θ_i over the resulting feature
266 maps leads to the definition of the following sets:
267

$$\begin{aligned} F_1 \cap F_2 &= \{x/\text{both channels are important for the fusion}\} \\ F_i &= \{x/\text{channel } i \text{ is important for the fusion}\} \\ \bar{F}_1 \cup \bar{F}_2 &= \{x/\text{no channel is important for the fusion}\} \end{aligned} \quad (3)$$

270 where θ_i sets up the difference between *important* and *not*
271 *important* on channel i .

272 The resulting sets can be related to the different levels of
273 the fuzzy measure defined in the image space (see Fig. 2).
274 Hence the intersection $F_1 \cap F_2$ is related to the coefficient
275 in the level 2, namely $\mu(A_1 \cup A_2)$, the sets F_i are related
276 to $\mu(A_i)$, and the union of the complements to $\mu(\emptyset)$. If the
277 goal to be achieved by partitioning the image space is the
278 increment of the flexibility of the fuzzy integral, the mono-
279 tonicity of the fuzzy measure has to be broken. This cannot
280 be achieved with just one measurable space as stated by Eq.
281 (2). Therefore the image space is divided in three different
282 subspaces \mathcal{C}^j through the mapping $X \rightarrow F \rightarrow \mathcal{C}^j \forall j =$
283 $1, 2, 3$, where three different fuzzy measures μ^j can be
284 defined. Thus these fuzzy measures can break the mono-
285 tonicity condition by presenting $\mu_{12}^1 \leq \mu_1^2$ and $\mu_{12}^1 \leq \mu_2^2$.

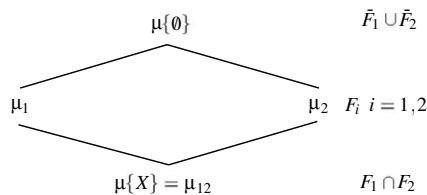


Fig. 2. Relationship among feature sets and levels in the lattice structure of a fuzzy measure which is used for deriving the expression of an ILFO.

286 The subspaces, where the different fuzzy measures μ^j are
287 localized, can be defined upon the following classes:
288

$$\begin{aligned} \mathcal{C}^1 &= \{F_1 \cap F_2\} \Rightarrow \mu^1 \\ \mathcal{C}^2 &= \{F_1 - (F_1 \cap F_2), F_2 - (F_1 \cap F_2)\} \Rightarrow \mu^2 \\ \mathcal{C}^3 &= \{\bar{F}_1 \cup \bar{F}_2\} \Rightarrow \mu^3 \end{aligned} \quad (4)$$

291 The set difference of the second class assures the classes to
292 be disjoint, i.e. each point can just belong to one class. The
293 generalization of these definitions for three channels is
294 depicted in Fig. 3. The class definitions for a larger number
295 of classes can be defined in an analogous manner. Here the
296 number of classes m is determined by the number of levels
297 to be singularly considered in order to overcome the mono-
298 tonicity of the fuzzy measure (see Fig. 2), being $m = n + 1$
299 and n the number of information sources.

300 The former definitions can be also generalized by apply-
301 ing the Fuzzy Set Theory [10]. This is attained by applying
302 a tolerance factor ε over the threshold θ (see Fig. 4). In this
303 case, the classes \mathcal{C}^j become fuzzy classes. Moreover the
304 points of the label image present so many membership
305 degrees as classes are defined, therefore becoming a fuzzy
306 label image. Hence, each point presents a membership
307 degree for each of the classes that will be denoted as ζ_j ,
308 $\forall j = 1, \dots, m$. The result of the ILFO is the linear combina-
309 tion of the fuzzy integrals for each class:
310

$$\text{ILFO}[h_1(x_1), \dots, h_n(x_n)] = \zeta_1 \mathcal{F}_{\mu^1} + \dots + \zeta_m \mathcal{F}_{\mu^m} \quad (5)$$

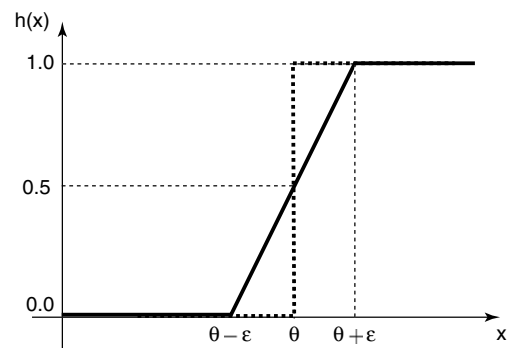


Fig. 4. Tolerance parameter ε for the fuzzification of the feature images in an ILFO with a fuzzy label image. The parameter turns the step function centered on θ (dotted line), which would have been used as threshold for the generation of a crisp label image, into a ramp-shaped fuzzy membership function (continuous line).

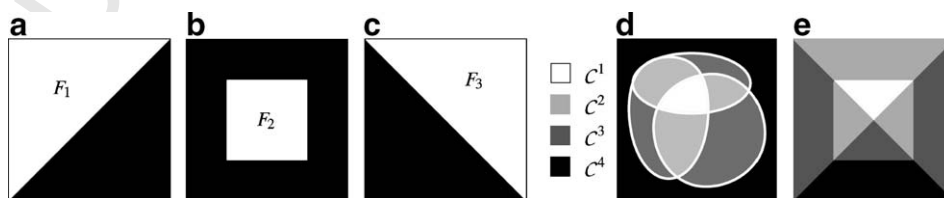


Fig. 3. Set diagram for the generation of a label image to be used in an ILFO, exemplary shown for three input channels. The process is based on the following set and class definitions: $F_i = \{x_i/\text{presents computed feature}\} \forall i = 1, 2, 3$; $\mathcal{C}^1 = \{F_1 \cap F_2 \cap F_3\}$; $\mathcal{C}^2 = \{(F_1 \cap F_2) - \mathcal{C}^1, (F_1 \cap F_3) - \mathcal{C}^1, (F_2 \cap F_3) - \mathcal{C}^1\}$; $\mathcal{C}^3 = \{F_1 - \mathcal{C}^2, F_2 - \mathcal{C}^2, F_3 - \mathcal{C}^2\}$; $\mathcal{C}^4 = \{\bar{F}_1 \cup \bar{F}_2 \cup \bar{F}_3\}$. (a-c) Binary maps resulting from the binarization of the corresponding feature map. (d) Venn diagram of the class definition. (e) Resulting label image.

313 where \mathcal{F}_μ states for any fuzzy integral (although the CFI
314 equation (1) is herein taken into consideration).

315 3.2. ILFOs' framework

316 The following section presents the framework of a gen-
317 eric ILFO. The implementation of an ILFO is composed
318 by three different modules: *LabImGen*, which generates
319 the label image where the fuzzy measures are localized,
320 *FuzMeCo*, which constructs these measures, and *FuzFus*,
321 which implements the expression given in Eq. (5). Since
322 the implementation of the module *FuzMeCo* is application
323 dependent, just the implementation of the label image gen-
324 eration is elucidated in the following paragraphs. The
325 reader is referred to [5] for an extended description of the
326 generic framework.

327 The block diagram of the module used for the genera-
328 tion of the label image (*LabImGen*), which was formally
329 defined in Section 3.1, is shown in Fig. 5. The different
330 modules are described in the following paragraphs.

331 Through the *FeatExt* module a particular feature of the
332 image is analyzed and characterized. A numerically
333 expressed feature is extracted from each of the input chan-
334 nels in this feature stage. This feature characterizes the
335 importance of the channel for the fusion result. Examples
336 of such a characterization could be the extraction of a blur-
337 ring coefficient or of the areas with low luminance.

338 In the binarization stage, which is implemented through
339 the module denoted as *Binar*, each of the feature distribu-
340 tion maps is binarized with θ_i . The parameter θ_i represents
341 the point up to which the feature evaluated on the channel
342 x_i is considered to be important enough in order to influ-
343 ence the fusion result. Thus the resulting binary maps rep-
344 resent this importance through a binary variable (see
345 Fig. 3a-c). Furthermore this module implements the set
346 definition of F_i as expressed by Eq. (3).

347 The purpose of the expert system (in the module *Exp-*
348 *Sys*) is the computation of the classes for the definition of
349 the different fuzzy measures as stated for instance in Eq.
350 (4). The expert system generates the binary images whose
351 true values indicate whether (and where) the feature is
352 important in the first channel, in the second channel, in

the first and second one, and so forth, etc. Afterwards
these sets are grouped in the different classes by applying
the corresponding logical operators, i.e. AND, OR, and
NOT.

The last module *Codif* takes the binary maps of the former
module as input. *Codif* generates the label image (see
Fig. 3e) by codifying the image points of each class j with
a grayvalue g_j . The outgoing label image is used for the
computation of the ILFO as already described.

If a fuzzy label image is generated, the module *Binar* is
substituted by a fuzzification module that implements the
fuzzification of the feature images with the monotonic
increasing fuzzy membership function defined by the toler-
ance value ε (see Fig. 4). The fuzzification module delivers a
set of fuzzy images to the expert system. Therefore the rule
system (*ExpSys*) becomes a fuzzy rule system. The treat-
ment of the fuzzy images resulting from the fuzzification
stage are operated in this case with T-norm, S-norm and
fuzzy complement operators [21].

The output of the procedure changes as well in this fuzzy
implementation. A set of fuzzy images, which constitute the
fuzzy label image, is delivered together with the crisp label
image (see Fig. 9 for an exemplary comparison between the
two approaches). The membership degrees contained in
these fuzzy images will be used as the real coefficients ζ_j
in the linear combination expressed in Eq. (5).

4. Application of ILFOs in a framework for highlights filtering

As formerly elucidated, the ILF paradigm can then be
applied in the implementation of the pre-processing frame-
work for the automated visual inspection of objects that
present highly reflective surfaces [5]. The presence of so-
called highlights, areas where the camera detector is satu-
rated, constitute the principal problem in the inspection
of these objects. Highlight areas are characterized by the
absence of visual information about the object structure.
Therefore a set of images, where complementary visual
information about the inspected object is contained, is gen-
erated in the image acquisition stage. Thence an ILFO is

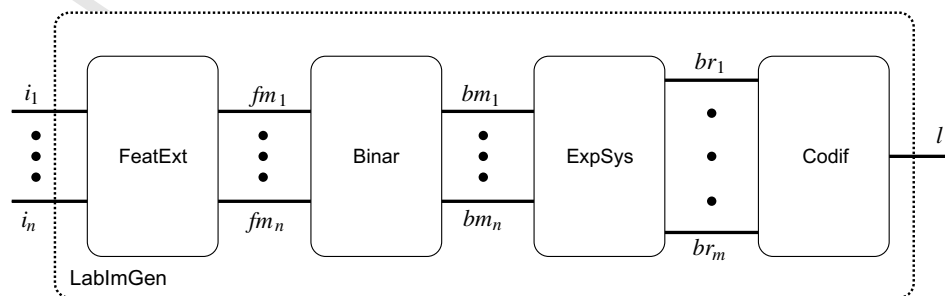


Fig. 5. Block diagram for the generation of a crisp label image in an ILFO. Signals. i_i : Input channels. fm_i : Features maps. bm_i : Binary feature maps. br_i : Binary class maps for different relationships. l : Crisp label image. Modules. *FeatExt*: Feature extraction. *Binar*: Binarization. *ExpSys*: Expert system. *Codif*: Codification.

392 applied on the acquired images in order to suppress the
393 highlight areas.

394 4.1. Image acquisition

395 Different images of the underlying object are taken with
396 a camera from the same position but with different adjust-
397 ments and illumination conditions. The image acquisition
398 stage attains the generation of an image set, where the
399 reflections appear in different positions and spatial exten-
400 sions. The less redundancy among these images, the better
401 result can be attained. Indeed the reflection areas with no
402 structure information cannot be filtered out and therefore
403 the underlying object information cannot be recovered [5].

404 The image acquisition is not trivial. Since the objects
405 being inspected present highly reflective surfaces, the reflec-
406 tion of the environment on them cannot easily be avoided.
407 Therefore the image acquisition stage should succeed by
408 protecting the camera, the lighting system, and the
409 inspected item from external lights. No other restrictions
410 concerning the surface structure¹ neither the reflection
411 properties have been detected hitherto. Moreover three
412 equal infrared lighting sources have been used in the acqui-
413 sition of the input image set employed. Thus three images
414 are generated for each item being inspected in the work
415 presented herein. The generation of a larger image set
416 can improve the pre-processing result. Thus more complex
417 acquisition systems, similar to this used in the generation of
418 the Amsterdam Library of Object Images database [22],²
419 can be used in order to acquire a less redundant image set.

420 4.2. Generation of the label image

421 Once the image set has been generated, the label image
422 for the fusion is computed (*LabImGen*). This is attained
423 through the application on the input images of the modules
424 depicted in Fig. 5 (or its fuzzy implementation). In the fil-
425 tering of highlights the feature to be extracted characterizes
426 areas with high luminance values. Therefore the grayvalue
427 of the input channels can be used itself as feature. A thresh-
428 old θ_i is applied on the grayvalue input channels in order to
429 determine the spatial distribution of the highlights on each
430 individual channel x_i .

431 A procedure used in the generation of the label image is
432 implemented for finding out the threshold θ_i on the feature
433 maps' histograms, whereby the determination of this
434 parameter is automated. The selected algorithm is part of
435 the watershed transformation for the segmentation of mul-
436 tidimensional histograms [12]. It is based on the concept of
437 dynamic of histogram peaks [23], which can be applied on

the local extrema of an histogram in order to filter out the
less representative ones.

438
439
440 The application of this procedure can be described as
441 follows. First all the local maxima of the inverted histo-
442 gram are selected (see Fig. 8a). Thence the values of these
443 maxima are sorted in descending order. The dynamic of
444 each local maximum is computed by going through the his-
445 togram till the maximum that occupies the next position in
446 the sorted list has been reached. The dynamic value of the
447 outgoing local maximum equals the difference between its
448 value and the minimum value encountered in the way to
449 the next maximum. This operation is repeated for all local
450 maxima in the histogram. The peak with the largest
451 dynamic among those with the larger grayvalue is selected
452 as the threshold θ_i in the application on hand (see the exem-
453 plary value in Fig. 8a).

454 Once the highlights have been found for all the input
455 channels, the label image itself is generated by the corre-
456 sponding rule system and the posterior codification. The
457 label image codifies then all the different highlights combi-
458 nations: no highlights, highlight in the first image, highlight
459 in the first and second image, etc.

460 4.3. Construction of fuzzy measures

461 A process for the determination of the fuzzy measures is
462 thence undertaken (*FuzMeCo*). The number of different
463 labels in the label image m fixes up how many fuzzy mea-
464 sures have to be constructed. genetic algorithms [13] and
465 Interactive genetic algorithms are employed [14] for this
466 purpose herein.

467 4.3.1. Genetic algorithms

468 The characteristic function of Evolutionary Computing
469 is the computation of a solution in non-linear optimization
470 problems [24]. Genetic algorithms have been successfully
471 used for constructing fuzzy measures [25–27]. The fuzzy
472 measure coefficients are first encoded by arrays of real
473 numbers. The general methodology of genetic algorithms
474 with standard operators [13] applies for this problem.
475 The iterative search is driven by a so-called fitness function,
476 which characterizes the optimality of the individual solu-
477 tions in each step.

478 In the here presented application of genetic algorithms
479 three different fitness functions $f_i(x)$, which were proposed
480 in [5], are evaluated. The first function (f_1) presents the fol-
481 lowing expression:
482

$$483 f_1(x) = 0.8\sigma_g^2 + \sum_{i=0}^{N-1} [0.75h_b(g_i) + 0.2h_d(g_i)] \quad (6) \quad 484$$

485 where N states for the number of pixels of the final image,
486 σ_g^2 denotes the variance of the grayvalues, and h_b and h_d ,
487 two fuzzy functions that count the number of pixels with
488 respectively a maximal and minimal grayvalue g_i . The min-
489 imization of this function attains the minimization of the
490 number of pixels with extreme grayvalues. The weights of

¹ Obviously the complexity of the 3D structure hinders the visibility of all surfaces of an object, but this is not directly related to the highlights filtering.

² The database and some information about the employed acquisition system can be found at <http://www.science.uva.nl/~aloi/>.

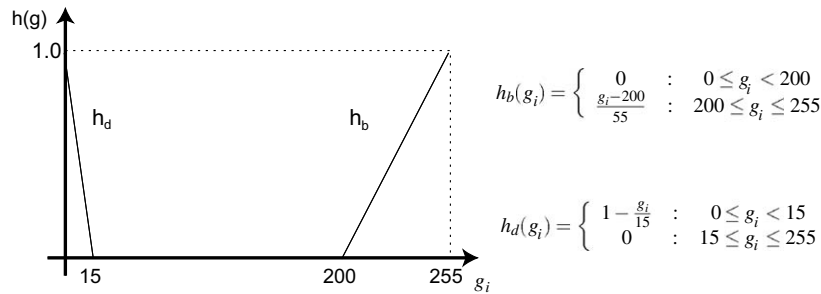


Fig. 6. Fuzzy membership functions used for image quality assessment used in the fitness function (6). The fuzzy membership function $h_b(g_i)/h_d(g_i)$ accounts for the pixels with a low/large grayvalue g_i . The lower/larger the grayvalue, the larger the weighting in the sum.

491 the three factors were heuristically found. The used trian-
492 gular fuzzy membership functions, h_b and h_d , are depicted
493 in Fig. 6 beside their mathematical expressions.

494 The grayvalue distribution of the fused image is driven
495 to present $\bar{g} = 128$ and $\sigma_g = 64$ by applying the second fit-
496 ness function (f_2), which is mathematically expressed as
497

$$499 f_2(x) = \|\bar{g} - 128\| + 2\|\sigma_g - 64\| \quad (7)$$

500 This expression drives the resulting image to present a
501 “standard” histogram.

502 The third fitness function (f_3) pursues a minimization of
503 the number of extreme grayvalues in the resulting image,
504 which is characterized by σ_g^2 :
505

$$507 f_3(x) = \sigma_g^2 \quad (8)$$

508 4.3.2. Interactive genetic algorithms

509 Interactive genetic algorithms are employed as an alter-
510 native to GAs for the implementation of *FuzMeCo*. The
511 application of interactive genetic algorithms allows evalu-
512 ating the final result directly by a user, avoiding the com-
513 plex determination of a fitness function [14].

514 The fitness computation is substituted by the presenta-
515 tion of the final image result for each individual to the user.
516 Thus the surface of the displaying monitor limits the num-
517 ber of individuals of the population. Populations of
518 between 10 and 20 individuals are used. The user interac-
519 tively selects the best results. These results are then used
520 for producing the next generation and the process is itera-
521 tively repeated. The number of generations is strong lim-
522 ited by the concentration capability of the user. Hence
523 the process takes about half an hour to be completed.

4.4. Fuzzy information fusion

525 Once the values of the fuzzy measure coefficients have
526 been determined, the fuzzy integral is applied on each pixel
527 of the multi-dimensional image set with respect to the fuzzy
528 measure codified in the label image (*FuzFus*). The result is
529 an image, where the highlight areas have been filtered out.

5. Application results

531 In the following sections the performance of different
532 systems for the automated visual inspection is analyzed.
533 The systems attain the inspection of different objects that
534 present highly reflective surfaces, namely: automotive
535 headlamp reflectors, consumer goods with plastic bundles,
536 and electric bulbs. The framework formerly described is
537 applied for the pre-processing of the generated images.
538 The results related to the highlights filtering are presented.

5.1. Inspection of headlamp reflectors

540 The presence of mirror-like surfaces makes the auto-
541 mated visual inspection of automotive headlamp reflectors
542 extremely complex. Therefore the presented pre-processing
543 framework is applied. The images generated are shown in
544 Fig. 7. In the following, different aspects of the system
545 are analyzed in detail.

5.1.1. Generation of the label image through peak dynamics analysis

546 The process for the generation of the label image is auto-
547 mated by first applying the analysis of the peak dynamics
548
549

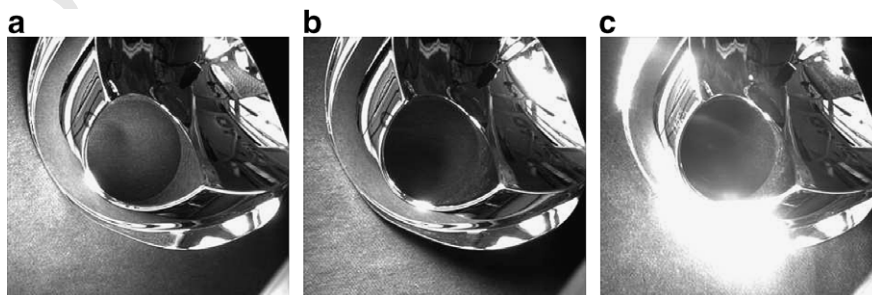


Fig. 7. Input images of the pre-processing stage of a system for the detection of structural faults on automotive headlamp reflectors (item I).

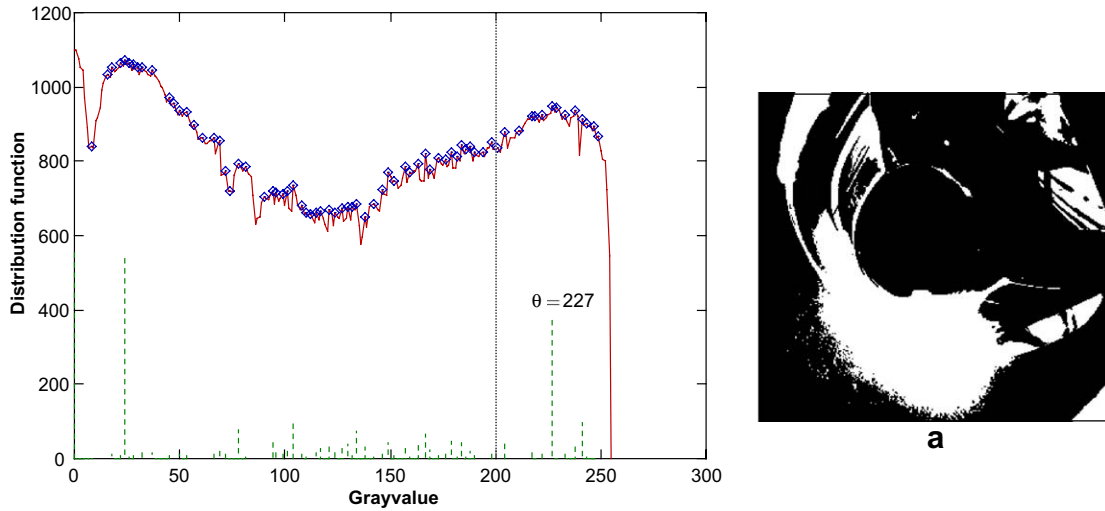


Fig. 8. Exemplary result of the computation of the peak dynamic (green dotted lines) of each local maximum (blue diamonds) on the inverted histogram (red continuous line) of the image shown in 7c. (a) Resulting binarization. (For interpretation of references in colour in this figure legend, the reader is referred to the web version of this article.)

550 in the image histograms, which delivers the value of the
 551 threshold θ_i for each input channel. The result of the peak
 552 dynamics analysis and the corresponding binarization are
 553 shown in Fig. 8.

554 The binary images obtained through the automated
 555 parametrization, are depicted in Fig. 9a–c. Furthermore
 556 the generation of the label image follows the mathematical
 557 framework given in Section 3.1 both in its crisp and fuzzy
 558 implementations. The resulting label image, and the fuzzy
 559 label images for $\varepsilon = 50$ can be seen in Fig. 9d–h.

5.1.2. Construction of the fuzzy measures through IGAs 560

561 An interactive genetic algorithm is used for the construc-
 562 tion of the fuzzy measures leading to the avoidance of high-
 563 lights in the fused image. The simulation is undertaken on
 564 the images shown in Fig. 7. It pursues the performance eval-
 565 uation of IGAs by comparing the results with those obtained
 566 through the application of GAs, which are presented in Sec-
 567 tion 5.1.3. The obtained results are shown in Fig. 10.

568 The interactive genetic algorithm strategy is tested with
 569 different parameterizations and different types of fuzzy

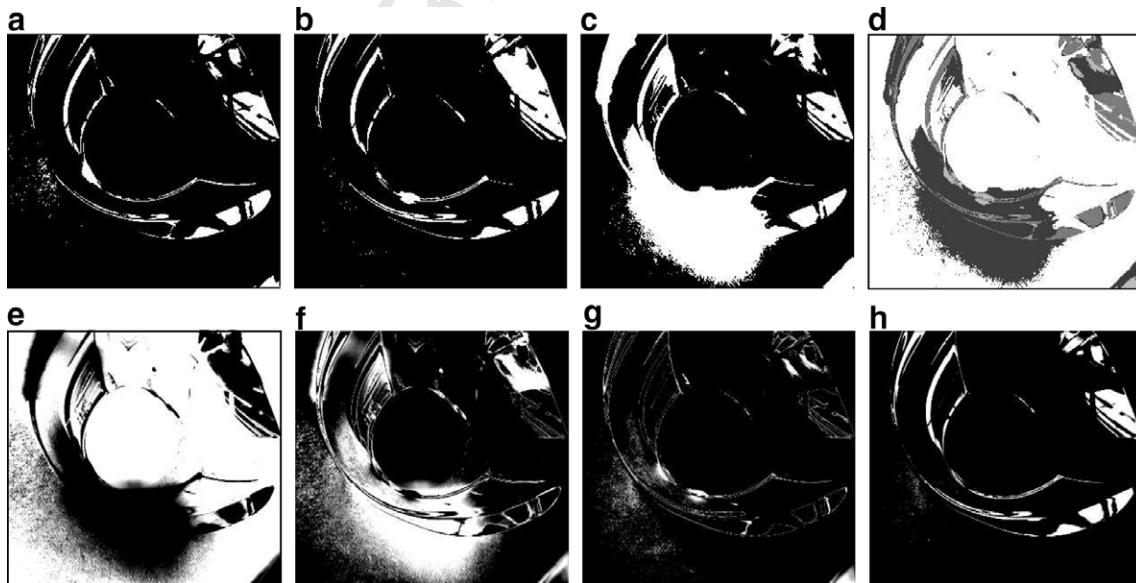


Fig. 9. Results of the binarization, the label image generation, and the fuzzy label image generation after automated determination of thresholds. Results of the binarization, the label image generation, and the fuzzy label image generation after automated determination of thresholds θ_i . (a) Binarization of image in Fig. 7a with $\theta_1 = 243$. (b) Binarization of image in Fig. 7b with $\theta_2 = 225$. (c) Binarization of image in Fig. 7c with $\theta_3 = 227$. (d) Resulting crisp label image. Fuzzy label image with fuzzy membership functions characterizing areas with: (e) no highlight, (f) highlight in one channel, (g) highlight in two channels, and (h) highlight in all three channels.

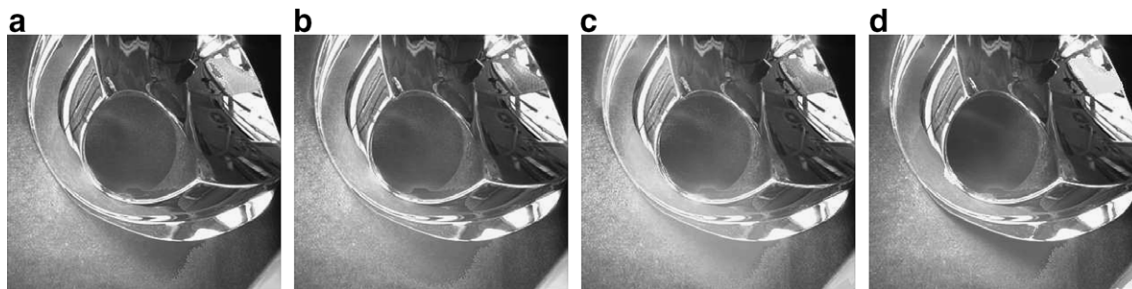


Fig. 10. Results of the utilization of interactive genetic algorithms for the construction of fuzzy measures. Results obtained on images depicted in Fig. 7 for different types of interactive genetic algorithms and different parametrizations (see Table 1).

Table 1

Type and parametrization of different interactive genetic algorithms used in the computation of the preliminary results depicted in Fig. 10

Fig. 10	GA type	Gen	PCross	PMut	El/PRapl	MType
(a)	Simple	20	0.8	0.1	Elitism	λ
(b)	StSt	8	0.95	0.1	0.9	λ
(c)	StSt	9	0.7	0.048	0.9	λ
(d)	StSt	10	0.81	0.024	0.9	General

Gen: number of generations. PCross: crossover probability. PMut: mutation probability. El: elitism. PRapl: replacement probability. MType: fuzzy measure type. StSt: steady state.

measures (see Table 1). The number of individuals is limited to 10 in order for all of them to fit in the displaying surface of a 17 in. computer monitor. The diversity among the individuals quickly decreases in each generation, i.e. the individuals tend to be equal up to the fifth generation. Although this shortcoming can be controlled (though cannot be avoided) through the crossover and mutation probabilities, this relationship does not seem to be deterministic. The interactive determination becomes tedious for the user up to the seventh generation. The utilization of an estimation of the fitness of each individual, which can then be modified by the user, improves the results (see Fig. 10c–d). The convergence of the genetic search in this case succeeds in a smaller number of generations than in the case where the user “blindly” gives the fitness of each individual (see Fig. 10a–b). The interactive parametrization process described in this section was undertaken by one user.

5.1.3. Construction of the fuzzy measures through GAs

A second simulation pursues the determination of the best GA’s parameterization in the construction of the fuzzy measure. Thus a genetic algorithm with different crossover and mutation probabilities are taken into consideration. The genetic algorithm is of type steady state, i.e. a percentage of the population, which is determined by the probability of replacement, is maintained over the different generations. The analysis is conducted for the fitness functions f_1 , Eq. (6), f_2 , Eq. (7), and f_3 , Eq. (8). The evolution of these fitness functions for the best individual of the population in each generation is analyzed for three values of crossover probability and four of mutation probability.

The evolution of each fitness function reaching the absolute minimum of all these combinations is depicted in Fig. 11.

Table 2 summarizes the best parameters resulting from the application of each fitness function. The evolution of the fitness function f_1 , Eq. (7), does not show any difference among the different values of mutation probability up to a particular number of generations (see Fig. 11b). In this case the fuzzy measures were selected after a subjective evaluation of the resulting images for the last generation.

The fuzzy measure coefficients obtained through the GAs parameterized as stated in Table 2 are selected. Thence the final results are computed (see Fig. 12) based on this parametrization.

5.1.4. Computational cost of the framework’s application and the influence of the tolerance factor (ε) on it

The computational cost of the framework presented herein has been analyzed on a computer with a PowerPC G3 processor working at 400 MHz with an implementation developed in Python, an interpreter programming language.³ The result of this analysis is shown in Fig. 13. The framework operates at approximately 0.1 ms per pixel, if it uses a “crisp” label image. Thus an image of 256×256 pixels is pre-processed in approximately 6.5 s for this configuration.

The execution time of the framework linearly varies with the increment of the tolerance ε (see Fig. 13a). Therefore a trade-off among the value of this parameter and the quality of the system’s output have to be undertaken. As it can be observed by comparing Figs. 13b and 12f, a larger tolerance does not necessarily imply a better performance of the system.

5.1.5. Generalization capability of the framework

Fig. 14 shows the input images generated over another object as the one considered so far. An ILFO with the same fuzzy measures found for the object considered up to now is applied on these input images. The results obtained for different fitness functions are depicted in Fig. 15. Taking into consideration that the results are achieved by applying

³ Interpreter languages are supposed to operate approximately 10 times slower than compiling ones.

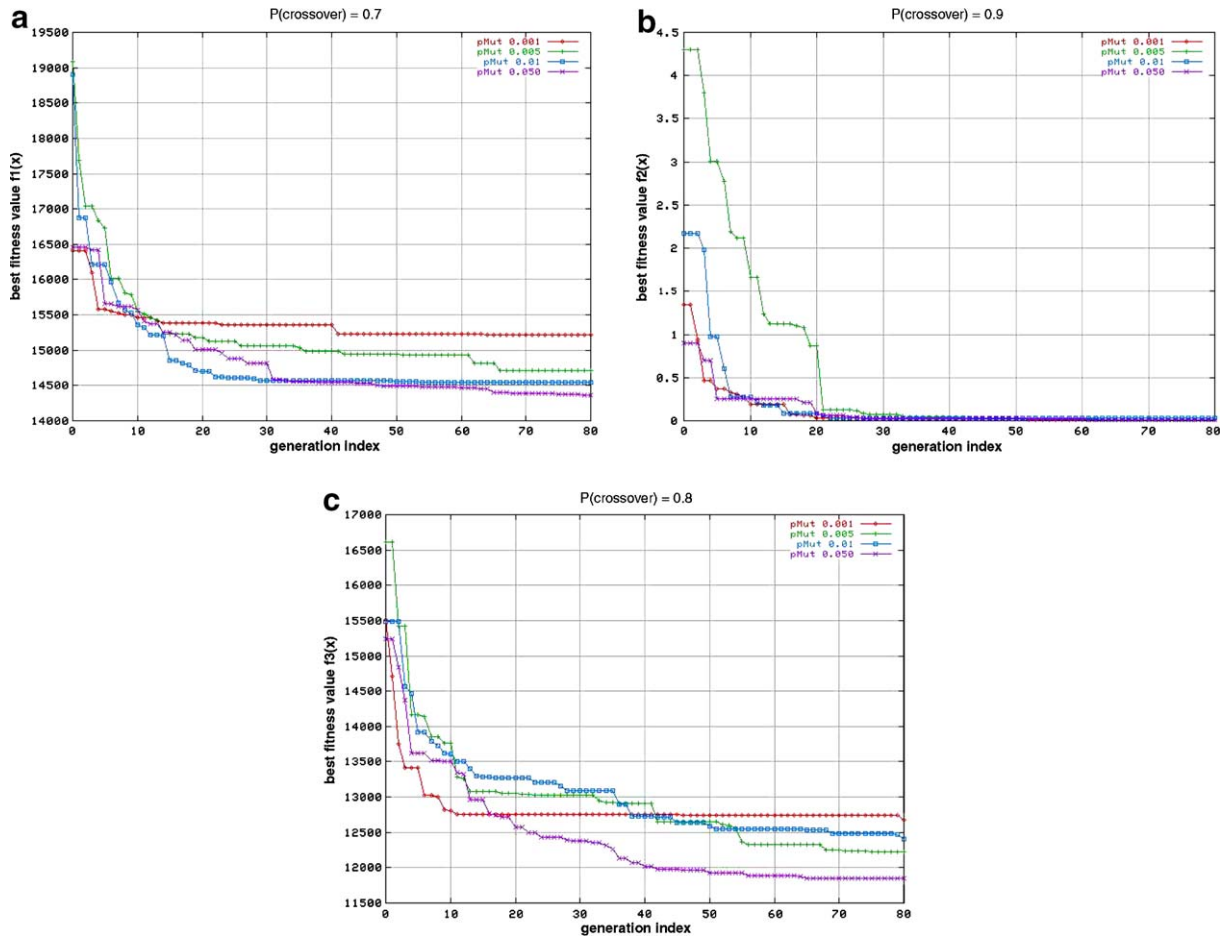


Fig. 11. Convergence of the GA over different generations in the computation of the fuzzy measure coefficients of the ILFO applied for obtaining the images depicted in Fig. 12(a-c). The convergence is shown for the best crossover-mutation combination of each considered fitness function $f_i(x)$ computed for the best individual in each generation. (a) Fitness function f_1 Eq. (6). (b) Fitness function f_2 Eq. (7). (c) Fitness function f_3 Eq. (8).

Table 2
Best parametrization of a steady state genetic algorithm for the construction of a fuzzy measure for different fitness functions f_i .

Parameter	f_1 Eq. (6)	f_2 Eq. (7)	f_3 Eq. (8)
Crossover probability	0.7	0.9	0.8
Mutation probability	0.05	0.005	0.05
Replacement probability	0.9	0.9	0.9
Number of generations	80	63	65
Population size	40	40	40
Result in Fig. 12	(a), (d)	(b), (e)	(c), (f)

638 the same conditions in the acquisition of the input images,
639 this simulation gives a clear idea of the generalization capa-
640 bility of the here presented framework.

641 5.1.6. Objective quality assessment of fusion results

642 The quality of the fusion results could be formerly
643 assessed from a subjective point of view (see Figs. 10 and
644 12). In this section different quality measures would be
645 applied on those results in order to objectively quantize
646 the performance of the framework presented herein. Three
647 different measures have been computed.

648 First the *weighted fusion quality* and the *edge-dependent*
649 *fusion quality* indices from [28] are taken into account.
650 These indices are based on the *image quality index* pro-
651 posed in [29], which reflects the local similarity and the
652 local luminance distortion between two images. This mea-
653 sure is adapted to the problem of image fusion in [28] by
654 applying some features of human perception. Hence the
655 dependence of the quality on the saliency of image elements
656 becomes a weighting factor in the *weighted fusion quality*
657 *index*. Moreover the importance of edge detection drives
658 the value of the *edge-dependent fusion quality index*.

659 On the other hand, the *mutual information index* [30] is
660 based on the computation of the mutual entropy among
661 different images. Therefore this index can be understood
662 as a statistical quality measure among image histograms,
663 where the spatial distribution of grayvalues does not play
664 any role. Nevertheless, this measure has been successfully
665 applied in the quality assessment of medical images' fusion.
666 The values of the mentioned quality measures are summa-
667 rized in Table 3.

668 The numerical results confirm the subjective inspection.
669 Hence the best results were obtained for the GA paramete-
670 rization in contrast with the IGA one. Furthermore the

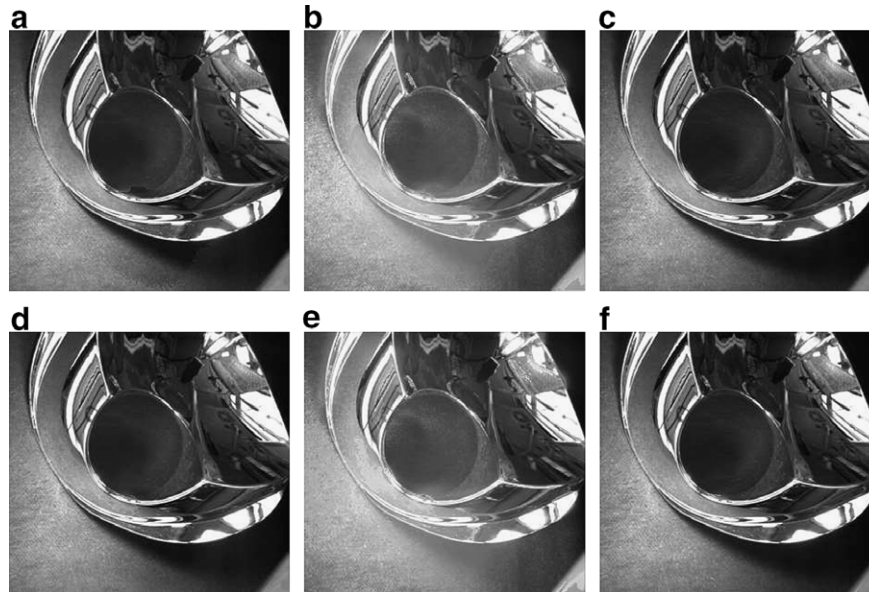


Fig. 12. Final results of an automated system for the visual inspection of headlamp reflectors, where the fuzzy measures are constructed after a GA with different fitness functions and parameterized according to Table 2. The results are obtained for two highlight tolerance (ϵ) values (see Section 3.2). (a) Fitness function f_1 Eq. (6) and $\epsilon = 0$. (b) Fitness function f_2 Eq. (7) and $\epsilon = 0$. (c) Fitness function f_3 Eq. (8) and $\epsilon = 0$. (d) Fitness function f_1 Eq. (6) and $\epsilon = 50$. (e) Fitness function f_2 Eq. (7) and $\epsilon = 50$. (f) Fitness function f_3 Eq. (8) and $\epsilon = 50$.

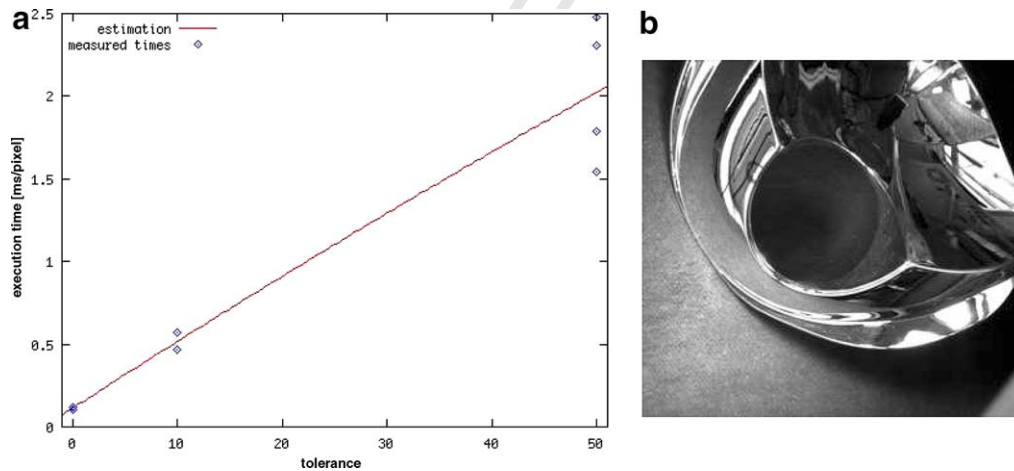


Fig. 13. (a) Estimation of the dependence of the execution time (ms/pixel) of an ILFO based on the CFI with respect to the highlight tolerance (ϵ) parameter (see Section 3.2). (b) Effect of the tolerance variation (ϵ) on the final results of the automated pre-processing system. Fuzzy measures are constructed after a GA with the fitness function f_3 (8) and parameterized according to Table 2. Highlight tolerance value $\epsilon = 10$ (compare with Fig. 12c and f).

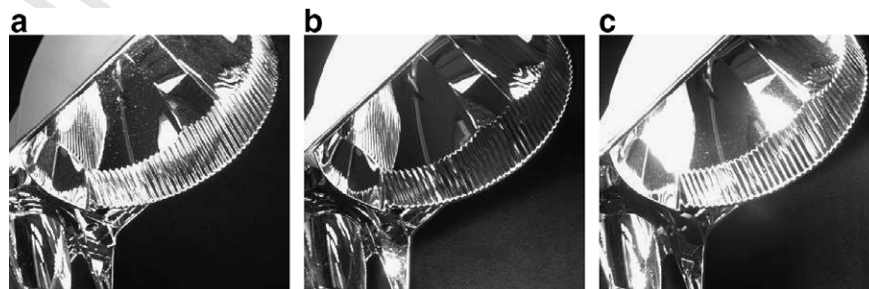


Fig. 14. Input images (of a second object) of the pre-processing stage in a system for the detection of structural faults on automotive headlamp reflectors (item II).

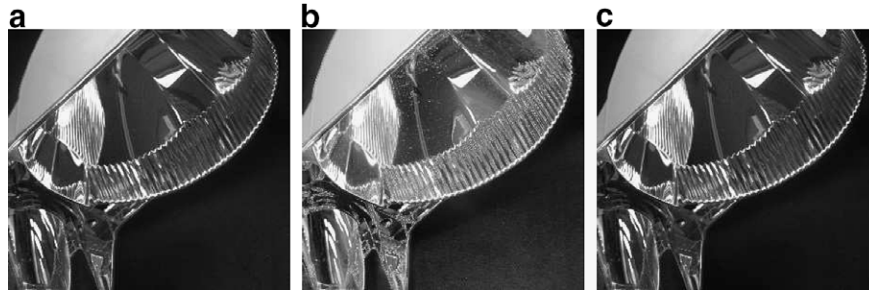


Fig. 15. Final results of the automated pre-processing system, where the fuzzy measures are obtained with a training on the object depicted in Fig. 7. (a) Fitness function f_1 Eq. (6). (b) Fitness function f_2 Eq. (7). (c) Fitness function f_3 Eq. (8).

Table 3

Objective comparison of fusion results through the application of three different quality measures, namely the *weighted fusion quality index* (Q_w) [28], *edge-dependent fusion quality index* (Q_E) [28], and the *mutual information index* (MI) [30], to some of the fusion results depicted in Figs. 10 and 12

	GA Fig. 12						IGA Fig. 10	
	f_1 Eq. (6)		f_2 Eq. (7)		f_3 Eq. (8)		Sim	StSt
	$\varepsilon = 0$	$\varepsilon = 50$	$\varepsilon = 0$	$\varepsilon = 50$	$\varepsilon = 0$	$\varepsilon = 50$		
Q_w	0.8446	0.8456	0.7971	0.8101	0.8198	0.8368	0.8166	0.7742
Q_E	0.6838	0.6857	0.5803	0.6015	0.6529	0.6758	0.6270	0.5493
MI	0.2653	0.2643	0.2313	0.2323	0.4096	0.2580	0.2335	0.2617
Fig.	12a	12d	12b	12e	12c	12f	10a	10d

The corresponding ILFOs were parameterized by applying: first genetic algorithms (GA) w.r.t. the three fitness functions f_i and two tolerance (ε) values; second two types of interactive genetic algorithms (IGA), namely based on a simple (Sim) and a steady state (StSt) GAs. Maximal values for each index are shown in bold typing.

671 fitness functions f_1 and f_3 perform better than f_2 . The
 672 results of these two fitness functions are similar. It is worth
 673 mentioning that following the numerical results the toler-
 674 ance factor is more important, when using f_1 . In this con-
 675 text the reader should take into account the increment in
 676 the computational cost that is associated with an increment
 677 of the tolerance value ε (see Section 5.1.4).

5.2. Inspection of plastic bundled packages

678

The automated inspection of a consumer good is pre-
 679 sented in this section (see Fig. 16). It shows the possible
 680 extension of the framework presented herein for the
 681 pre-processing of color images. The highlights are pro-
 682 duced by the plastic bundle of the object. Three different
 683

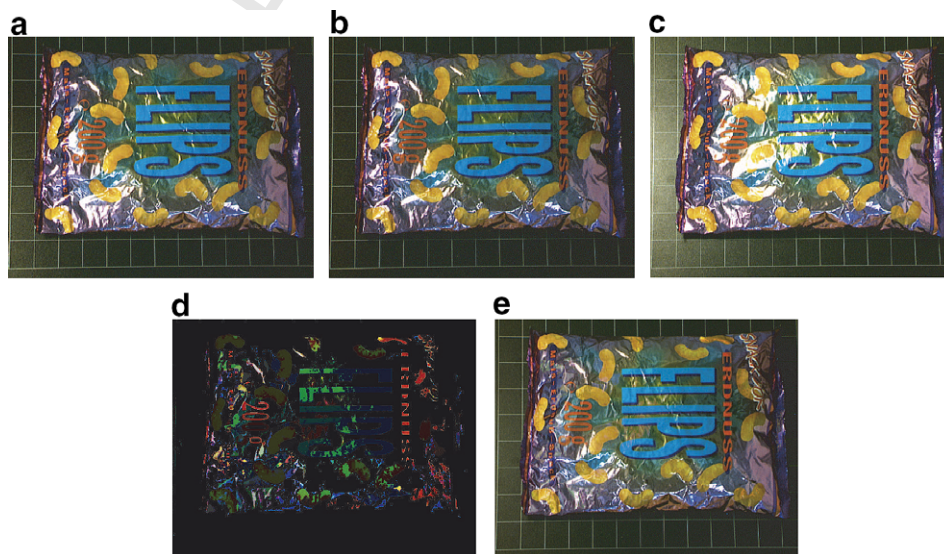


Fig. 16. Results of the extension of the framework presented herein for the pre-processing of color images in a market basket recognition prototype. (a-c) Input image set. (b) Label image. (c) Result of the application of an ILFO extended to color images.

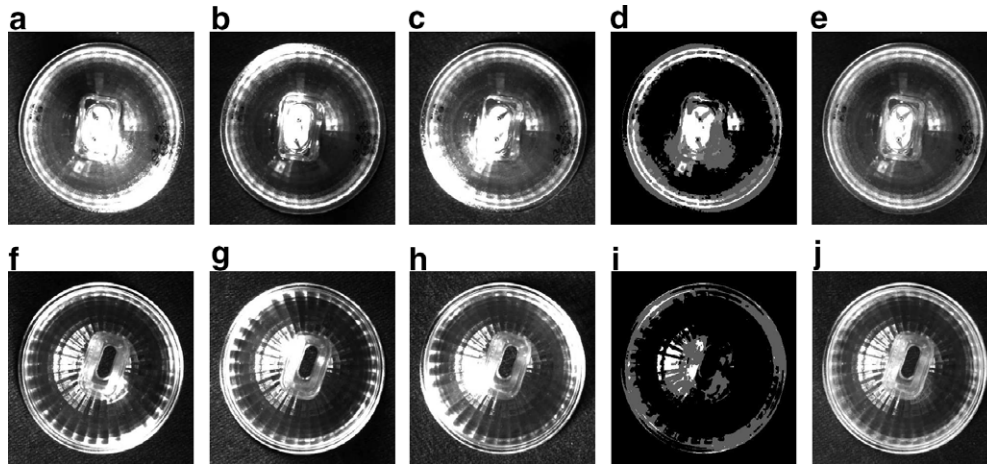


Fig. 17. Input images of the pre-processing stage in a system for the detection of structural faults on halogen bulbs.

684 images of the package are generated and depicted in
685 Fig. 16a–c.

686 The mentioned extension is achieved by applying an
687 ILFO to each of the color channels of the input image
688 set. First a mask is generated. The mask image, where
689 the fuzzy measures are localized, is depicted in Fig. 16d.
690 It is worth pointing out the limitation of the framework
691 w.r.t. to the inspection of free deformable objects (see
692 Fig. 16e). The pre-processing of such objects demands a
693 set of input images with larger cardinality. This increment
694 can reduce the number of redundant highlight areas among
695 the input images.

696 5.3. Inspection of halogen bulbs

697 The results obtained in the pre-processing of a structural
698 fault detection system, which was applied on halogen
699 bulbs, are described in the following. The input images of
700 the system are shown in Fig. 17a–c and f–h.

701 The generated mask images can be observed in Fig. 17d
702 and i. The obtained results are depicted in Fig. 17e and j.
703 The consequence of having redundant reflections on all
704 images of the input image set can be observed on the
705 depicted results. The reflection cannot be suppressed in
706 those areas where all images present one, since there is
707 no image information about the underlying structure. In
708 this case the redundant reflection, was caused by an external
709 light. The employed image acquisition module do not
710 use any protection against such influences. This one of
711 the shortcomings of the framework presented herein.

712 6. Conclusions

713 The framework for highlights filtering presented in [5]
714 has been systematically analyzed herein. Intelligent Local-
715 ized Fusion Operators, which generalize the employment
716 of the fuzzy integral for image fusion, are based on the local
717 definition of the fuzzy measures. Thus the formalization of

this operator, which is undertaken in this paper, allows
employing the operator as a pre-processing stage in different
automated visual inspection systems. Furthermore, the
results attained by such a pre-processing stage are
described. Particularly the utilization of peak dynamic analysis
as binarization procedure, the employment of Interactive
genetic algorithms and of genetic algorithms for the
parametrization of the fuzzy integral, and the generalization
capability of the framework, have been analyzed.

The application of an histogram analysis based on the
concept of peak dynamics demonstrates to be a very helpful
tool in the binarization of images corrupted by highlights
and therefore in the automation of the procedure. It is worth
mentioning that the values of the threshold θ automatically
obtained through the computation of the peak dynamics are
nearly the same as those heuristically set in [5] through the
visual analysis of the histograms.

The application of interactive genetic algorithms demonstrated
to be an interesting alternative to the application of genetic
algorithms. Nevertheless its usage should be improved for
obtaining satisfactory results. This fact was numerically proven
through the application on the resulting images of different
quality measures employed in image fusion. Since the best
parameterization of the genetic algorithms has been proposed
herein, this methodology remains hitherto the best option for
automatically defining the weighting parameters of the system.
The application of a fitness function minimizing the variance
of the grayvalue histogram outperforms other alternatives as
demonstrated both by the numerical analysis and the subjective
evaluation of the results obtained with this fitness function.
Therefore, its application allows the system to operate full
automated with a very good performance in the filtering of
highlights. The tolerance value ε constitutes the only free
parameter in the system. Taking the tolerance ε can become
helpful in the improvement of the results. Nevertheless a
performance trade-off between its computational cost and the
real improvement have to be undertaken in real appli-

756 cations. It is lastly worth pointing out that the results are
757 exclusively dependent on the acquisition adjustments, what
758 proves the generalization capability of the framework.

759 As it has been shown the performance of the pre-pro-
760 cessing system improves with the increment of the flexibil-
761 ity of the fusion operator. In this context Intelligent
762 Localized Fusion Operators offer novel possibilities for
763 solving challenging applications. The performance of the
764 pre-processing system can be improved by taking a more
765 systematic and controlled acquisition of images into con-
766 sideration. The utilization of a special illumination station
767 can allow the generation of a larger multi-dimensional
768 image set with less redundancy among the images of the
769 input image set. Furthermore the reflections of the environ-
770 ment on the object surfaces can be avoided in this fashion
771 as well. This is the most immediate goal to be attained in
772 the future in order to improve the pre-processing capability
773 of the system.

774 Acknowledgements

775 The author wants to thank: Jing Zhou, who completed
776 some of the here presented results, Daniel Kotow, who
777 ported part of the functionality of GALib to Python, and
778 Gemma Piella, who computed the quality measure of the
779 resulting images. My acknowledgement goes to the anony-
780 mous reviewers as well, whose comments on the manu-
781 script resulted very helpful in order to improve the
782 original text. The implemented software makes use of the
783 GALib genetic algorithm package (<http://lancet.mit.edu/ga/>),
784 written by Matthew Wall at the MIT, and Python
785 as prototyping language (<http://www.python.org>).

786 References

787 [1] P. Burt, R. Kolczynski, Enhanced image capture through fusion, in:
788 Proc. 4th Int. Conf. Computer Vision, ICCV, Berlin, Germany, 1993,
789 pp. 173–182.
790 [2] S. Yi, R.M. Harlick, L.G. Shapiro, Optimal sensor and light source
791 positioning for machine vision, Computer Vision and Image Under-
792 standing 61 (1) (1995) 122–137.
793 [3] F. Puente León, J. Beyerer, Datenfusion zur gewinnung hochwertiger
794 bilder in der automatischen sichtprüfung, Automatisierungstechnik 45
795 (1997) 480–489.
796 [4] S. Mann, Intelligent Image Processing, Wiley Interscience, New York,
797 2002.
798 [5] A. Soria-Frisch, Avoidance of highlights through ILFOs in auto-
799 mated visual inspection, in: M. Nachtgael, D. Van der Weken, D.
800 Van De Ville, E.E.E. Kerre (Eds.), Fuzzy Filters for Image Process-
801 ing, Springer-Verlag, 2003, pp. 356–371.
802 [6] J. Beyerer, F. Puente León, Suppression of inhomogeneities in images
803 of textured surfaces, Optical Engineering 36 (1) (1997) 85–93.
804 [7] M. Sugeno, The theory of fuzzy integrals and its applications, Ph.D.
805 thesis, Tokyo Institute of Technology, 1974.
806 [8] A. Soria-Frisch, Soft data fusion in image processing, in: R. Roy, M.
807 Köppen, S. Ovaska, T. Furuhashi, F.E. Hoffmann (Eds.), Soft-

Computing and Industry: Recent Advances, Springer-Verlag, 2002, 808
pp. 423–444. 809
[9] A. Soria-Frisch, Soft data fusion for computer vision, Ph.D. thesis, 810
Technical University Berlin, 2004. 811
[10] L.A. Zadeh, Fuzzy sets, Information Control 8 (1965) 338–353. 812
[11] S. Watanabe, Pattern Recognition: Human and Mechanical, John 813
Wiley & Sons, New York, 1985. 814
[12] P. Soille, Partitioning of multispectral images using mathematical 815
morphology, Vision Jahrbuch II (1993) 33–43. 816
[13] D.E. Goldberg, Genetic Algorithms in Search, Optimization and 817
Machine Learning, Addison-Wesley Pub. Co., Inc., Reading, Masa- 818
chusetts, 1989. 819
[14] H. Takagi, Interactive evolutionary computation: fusion of the 820
capabilities of EC optimization and human evaluation, Proceedings 821
of the IEEE 89 (9) (2001) 1275–1296. 822
[15] R.R. Yager, On ordered weighted averaging aggregation operators in 823
multicriteria decision making, IEEE Transactions on Systems, Man 824
and Cybernetics 18 (1) (1988) 183–190. 825
[16] R.R. Yager, A. Kelman, Fusion of fuzzy information with consid- 826
erations for compatibility, partial aggregation and reinforcement, 827
International Journal of Approximate Reasoning 15 (2) (1996) 93– 828
122. 829
[17] M. Grabisch, H.T. Nguyen, A.A. Walker, Fundamentals of Uncer- 830
tainty Calculi with Applications to Fuzzy Inference, Kluwer Aca- 831
demic Publishers, Dordrecht, Holland, 1995. 832
[18] M. Grabisch, J.-M. Nicolas, Classification by fuzzy integral: perfor- 833
mance and tests, Fuzzy Sets and Systems 65 (1994) 255–271. 834
[19] J.M. Keller, P. Gader, H. Tahani, J.-H. Chiang, M. Mohamed, 835
Advances in fuzzy integration for pattern recognition, Fuzzy Sets and 836
Systems 65 (1994) 255–271. 837
[20] A. Soria-Frisch, A new paradigm for fuzzy aggregation in multisens- 838
ory image processing, in: Computational Intelligence: Theory and 839
Applications, Proc. Int. Conf. 7th Fuzzy Days, 2001, pp. 59–67. 840
[21] E.P. Klement, R. Mesiar, E. Pap, Triangular Norms, Kluwer 841
Academic Publisher, Dordrecht, Holland, 2000. 842
[22] J.-M. Geusebroek, G.J.J. Burghouts, A.W. Smeulders, The Amster- 843
dam library of object images, International Journal of Computer 844
Vision 61 (1) (2005) 103–112. 845
[23] M. Grimaud, New measure of contrast: dynamics, Image Algebra and 846
Morphological Image Processing III 1769 (1992) 292–305. 847
[24] T. Furuhashi, Fusion of fuzzy/neuro/evolutionary computing for 848
knowledge acquisition, Proceedings of the IEEE 89 (9) (2001) 1266– 849
1274. 850
[25] T.-Y. Chen, J.-C. Wang, G.-H. Tzeng, Identification of general fuzzy 851
measures by genetic algorithms based on partial information, IEEE 852
Transactions on Systems, Man, and Cybernetics – Part B 30 (4) (2000) 853
517–528. 854
[26] G.J. Klir, Z. Wang, D. Harmanec, Constructing fuzzy measures in 855
expert systems, Fuzzy Sets and Systems 92 (1997) 251–264. 856
[27] Z. Wang, K.-S. Leung, J. Wang, A genetic algorithm for determining 857
nonadditive set functions in information fusion, Fuzzy Sets and 858
Systems 102 (1999) 463–469. 859
[28] G. Piella, H. Heijmans, A new quality metric for image fusion, in: 860
Proc. Int. Conf. Image Processing, ICIP, Band III, Barcelona, 861
Catalonia, 2003, pp. 173–176. 862
[29] Z. Wang, A. Bovik, A universal image quality index, IEEE Signal 863
Processing Letters 9 (3) (2002) 81–84. 864
[30] G. Qu, D.L. Zhang, P.F. Yan, Medical image fusion by wavelet 865
transform modulus maxima, Journal of the Optical Society of 866
America 9 (4) (2001) 184–190. 867
868